Shot-noise current-current correlations in multiterminal diffusive conductors

Ya. M. Blanter and M. Büttiker
Département de Physique Théorique, Université de Genève, CH-1211, Genève 4, Switzerland
(Received 28 January 1997)

We investigate the correlations in the current fluctuations at different terminals of metallic diffusive conductors. We start from scattering matrix expressions for the shot noise and use the Fisher-Lee relation in combination with diagram technique to evaluate the noise correlations. Of particular interest are exchange (interference) effects analogous to the Hanbury Brown–Twiss effect in optics. We find that the exchange effect exists in the ensemble-averaged current correlations. Depending on the geometry, it might have the same magnitude as the mean-square current fluctuations of the shot noise. The approach that we use is also applied to present a different derivation of the 1/3 suppression of shot noise in a two-terminal geometry, which is valid for an arbitrary relation between the length and wire width. We find that in all geometries correlations are insensitive to dephasing. [S0163-1829(97)03127-5]

I. INTRODUCTION

The shot noise in mesoscopic systems[1] continues to attract the attention of both theorists and experimentalists. For diffusive conductors, which are considered here, the two-terminal shot noise is studied quite well. The remarkable 1/3 suppression of the shot noise with respect to the Poisson value

$$S(\omega=0)=\frac{1}{3}eGV$$

[here, as usual, $S(\omega)$ is the Fourier transform of the current-current correlator, $S(t)=\langle\Delta I(t)\Delta I(0)\rangle$, while G and V are the conductance of the wire and the applied voltage, respectively; $\Delta I=I(t)-\langle I\rangle$] was derived in three different ways: from the distribution of transmission eigenvalues in a wire,[2] semiclassically from the Langevin equation,[3] and through a microscopic calculation of local current densities.[4] Later, Nazarov[5] claimed that this 1/3 suppression holds for an arbitrary two-terminal geometry (not necessarily quasi-one-dimensional). Subsequent to experiments by Liefrink *et al.*,[6] which demonstrated shot-noise suppression even for conductors much longer than the dephasing length, de Jong and Beenakker[7] provided a semiclassical discussion that showed that the 1/3 suppression is insensitive to dephasing. More recent experiments by Steinbach *et al.*[8] demonstrated the transition from the 1/3-suppression regime in wires short compared to an inelastic length through an interaction-dominated regime[9,10] to a regime where shot noise is suppressed by inelastic scattering.[2,11,12] A macroscopic metal exhibits no shot noise.[13]

Here we investigate the shot noise in mesoscopic diffusive conductors in a multiterminal geometry. Primarily, we focus on the interference experiment,[14] which is analogous to the experiment of Hanbury Brown and Twiss in optics.[15] Namely, we consider a conductor, connected to four reservoirs α, β, γ, and δ at equilibrium (Fig. 1), and discuss three types of experiments. In experiment A current is incident from the probe β, i.e., $\mu_\alpha=\mu_\gamma=\mu_\delta$ and $\mu_\beta-\mu_\alpha=eV$, μ_λ being the chemical potential of electrons in the reservoir λ. In experiment B current is incident from the probe δ: $\mu_\alpha=\mu_\beta=\mu_\gamma$ and $\mu_\delta-\mu_\alpha=eV$. Finally, in experiment C current is incident from both probes β and δ: $\mu_\alpha=\mu_\gamma$, $\mu_\beta=\mu_\delta$, and $\mu_\beta-\mu_\alpha=eV$. The current correlation in probes α and γ is measured in all the experiments, $S_j(t)=-\langle\Delta I_\alpha(t)\Delta I_\gamma(0)\rangle$, $j=A,B,C$.

The general analysis of Ref. 14 allows one to express

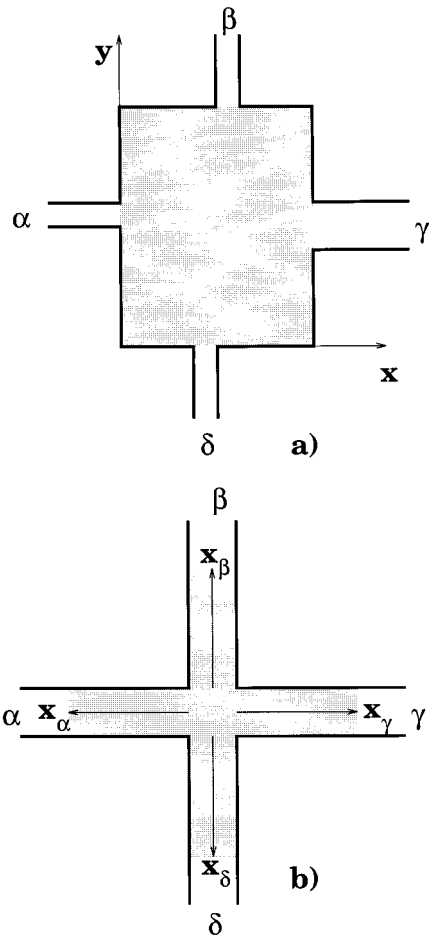

FIG. 1. Four-terminal conductors; the disordered area is shaded.

these quantities in terms of scattering matrices $\hat{s}^{\lambda\nu}$, with indices λ and ν labeling the probes. Thus, for zero frequency and temperature[16] one obtains

$$\begin{Bmatrix} S_A \\ S_B \\ S_C \end{Bmatrix} = \frac{e^2}{\pi} e|V| \begin{Bmatrix} \Xi_1 \\ \Xi_2 \\ \Xi_1+\Xi_2+\Xi_3+\Xi_4 \end{Bmatrix}, \tag{1}$$

with quantities Ξ_i defined as

$$\begin{aligned} \Xi_1 &= \mathrm{Tr}(s^{\dagger\alpha\beta} s^{\alpha\beta} s^{\dagger\gamma\beta} s^{\gamma\beta}), \\ \Xi_2 &= \mathrm{Tr}(s^{\dagger\alpha\delta} s^{\alpha\delta} s^{\dagger\gamma\delta} s^{\gamma\delta}), \\ \Xi_3 &= \mathrm{Tr}(s^{\dagger\alpha\beta} s^{\alpha\delta} s^{\dagger\gamma\delta} s^{\gamma\beta}), \\ \Xi_4 &= \mathrm{Tr}(s^{\dagger\alpha\delta} s^{\alpha\beta} s^{\dagger\gamma\beta} s^{\gamma\delta}). \end{aligned} \tag{2}$$

The scattering matrices are evaluated at the Fermi surface and the trace is taken with respect to channel indices.

Thus $S_C \neq S_A + S_B$: Experiments A and B are not additive due to the interference terms Ξ_3 and Ξ_4. It was shown in Ref. 14 that these terms have different signs for fermions and bosons; hence we will call them exchange terms. We define an exchange contribution as

$$\Delta S = S_C - S_A - S_B .$$

It follows from the unitarity of matrices $s^{\lambda\nu}$ that the quantities Ξ_1 and Ξ_2, which represent the classical result, are positively defined.[17] At the same time, traces Ξ_3 and Ξ_4 can have either sign: they are in fact not even real. This means that exchange interference may either suppress or enhance the classical value.

In a disordered system all these quantities should be averaged over impurity configurations. Naively, one might think that due to the phases contained in the quantities Ξ_3 and Ξ_4 these will average to zero and thus the average of the exchange term $\langle \Delta S \rangle$ vanishes (here angular brackets are used to indicate the disorder average). Below we explicitly calculate disorder-averaged correlation functions S_j and demonstrate that it is not the case. The average exchange correlator $\langle \Delta S \rangle$ generally has a nonzero value. An analysis of the exchange correlator for chaotic cavities, reported elsewhere,[18] leads to a similar conclusion.

The paper is organized as follows. First, we investigate disorder averages of scattering matrices starting from Eqs. (2) and using the Fisher-Lee relation, which connects scattering matrices and Green's functions. We then use diagram techniques developed for disordered systems to find the ensemble averages. As a simple check of the method developed, we give a derivation of the 1/3 suppression of the two-terminal shot noise for an arbitrary (not necessarily quasi-one-dimensional) geometry, thus confirming the result by Nazarov.[5] Then we turn to exchange-interference experiments and consider the two particular four-terminal geometries, shown in Fig. 1. We demonstrate that the geometry of Fig. 1(a) implies a negative exchange correlation, with the quantity ΔS being of the same order of magnitude as correlators S_A and S_B themselves. In contrast, the cross geometry of Fig. 1(b) shows a strong suppression of exchange effects and gives a positive sign of the latter, provided the motion through the center of a cross is ballistic. Otherwise the exchange effect is governed by the scattering inside the cross center only.

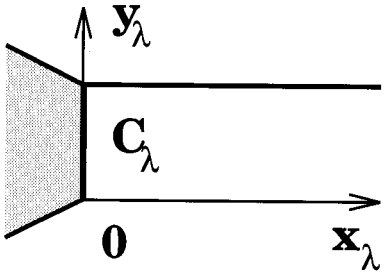

FIG. 2. Contact of a disordered region (shaded) with an ideal lead λ.

In the calculations below we disregard electron-electron interaction. The latter is known not to produce an essential effect on two-terminal shot noise[9,10] provided the wire is short in comparison to the inelastic scattering length. We will show that the origin for this is that in the ensemble-averaged quantities the effect is local and electron trajectories enclosing a large area are suppressed. This explains why the shot noise is not sensitive to dephasing. Hence we believe that electron-electron interactions are not important for the exchange effects in shot noise. Note, however, that nonlinear noise is affected by interactions, as was shown recently.[19] Interactions are also expected to affect the frequency dependence of the shot-noise power.

II. GENERAL FORMALISM AND TWO-TERMINAL SHOT NOISE

We consider a disordered two-dimensional system, connected to reservoirs by ideal leads. Transverse motion of electrons in each lead is quantized and we assume that all leads are wide, i.e., the number of transverse channels at the Fermi surface in the lead λ is large, $N_\lambda \sim p_F W_\lambda \gg 1$. Here p_F is the Fermi momentum, while W_λ is the width of the lead.

General relations[20–22] allow one to express scattering matrices for an arbitrary geometry through retarded and advanced Green's functions of the system. The standard procedure[22] is as follows. One chooses arbitrary cross sections of the leads C_λ and introduces local coordinates related to these cross sections (Fig. 2). Since none of the quantities discussed here depends on the choice of these cross sections, it is convenient to choose them as the boundary between disordered region and leads. One obtains

$$\begin{aligned} s_{mn}^{\lambda\nu}(E) = -\frac{i}{4M^2(v_m v_n)^{1/2}} \int_{C_\lambda} dy_\lambda \int_{C_\nu} dy_\nu G_E^R(\boldsymbol{r}_\lambda, \boldsymbol{r}_\nu)(\boldsymbol{D}_\lambda \hat{\boldsymbol{n}}_\lambda) \\ \times (\boldsymbol{D}_\nu \hat{\boldsymbol{n}}_\nu) \exp(-ik_m x_\lambda - ik_n x_\nu) \chi_m(y_\lambda) \chi_n(y_\nu) \end{aligned} \tag{3}$$

and

$$s^{\dagger\lambda\nu}_{nm}(E)=\frac{i}{4M^2(v_m v_n)^{1/2}}\int_{C_\lambda}dy_\lambda\int_{C_\nu}dy_\nu G^A_E(\boldsymbol{r}_\nu,\boldsymbol{r}_\lambda)(\boldsymbol{D}_\lambda\hat{\boldsymbol{n}}_\lambda)\times(\boldsymbol{D}_\nu\hat{\boldsymbol{n}}_\nu)\exp(ik_m x_\lambda+ik_n x_\nu)\chi_m(y_\lambda)\chi_n(y_\nu). \quad (4)$$

Here $v_m=k_m/M$, M being the effective electron mass. The longitudinal wave vectors in the lead λ are

$$k_m=[p_F^2-(\pi m/W_\lambda)^2]^{1/2}$$

and those in lead ν are denoted by k_n. Furthermore, $\hat{\boldsymbol{n}}_\lambda$ is the unit vector in the direction x_λ, while χ_m and χ_n are wave functions of transverse motion in the leads λ and ν, respectively; for simplicity we choose them to be real. Finally, $\boldsymbol{D}$ denotes a double-sided derivative

$$f\boldsymbol{D}g=f\nabla g-g\nabla f.$$

In principle, Eqs. (3) and (4) allow one to average arbitrary combinations of scattering matrices over disorder, using the standard diagram technique.[23] It seems that the approach outlined here has not been used so far for the (analytical) calculation of any physical properties. However, it is rather close to the Hamiltonian approach, employed extensively for the calculation of conductance and conductance fluctuations.[24–28] Below we demonstrate that our formalism reproduces the 1/3 suppression of two-terminal shot noise; in particular, as a simplest check, we also reproduce the Drude formula for conductance.

The rest of the section is devoted to the two-terminal geometry: a diffusive wire of the length L and width W, connected to two ideal leads α and β; $L,W\gg l$, with l being the mean free path. For a moment we also assume $L\gg W$, a restriction that eventually will be lifted. We introduce an axis $\hat{x}$ directed along the wire, $0\leqslant x\leqslant L$, and an axis $\hat{y}$ directed across the wire. The general expressions (3) and (4) can be rewritten as

$$s^{\alpha\beta}_{mn}(E)=\frac{i}{4M(k_m k_n)^{1/2}}\int_{C_\alpha}dy_1\chi_m(y_1)\int_{C_\beta}dy_2\chi_n(y_2)\times[-\partial_{x_1}+ik_m][-\partial_{x_2}-ik_n]G^R_E(\boldsymbol{r}_1,\boldsymbol{r}_2)\big|^{x_1=0}_{x_2=L} \quad (5)$$

and

$$s^{\dagger\alpha\beta}_{mn}(E)=-\frac{i}{4M(k_m k_n)^{1/2}}\int_{C_\alpha}dy_1\chi_n(y_1)\int_{C_\beta}dy_2\chi_m(y_2)\times[-\partial_{x_1}-ik_n][-\partial_{x_2}+ik_m]G^A_E(\boldsymbol{r}_2,\boldsymbol{r}_1)\big|^{x_1=0}_{x_2=L}. \quad (6)$$

Two-terminal shot-noise power $S\equiv S(\omega=0)$ can be conveniently expressed through scattering matrices evaluated at the Fermi level,[29,30]

$$S=\frac{e^2}{2\pi}eV\langle\mathrm{Tr}[s^{\dagger\alpha\beta}s^{\alpha\beta}]-\mathrm{Tr}[s^{\dagger\alpha\beta}s^{\alpha\beta}s^{\dagger\alpha\beta}s^{\alpha\beta}]\rangle. \quad (7)$$

Note that the first trace on the right-hand side is related to the conductance

$$G=\frac{e^2}{2\pi}\langle\mathrm{Tr}[s^{\dagger\alpha\beta}s^{\alpha\beta}]\rangle.$$

It is convenient to calculate both traces separately.

A. Evaluation of $\langle\mathrm{Tr}[s^{\dagger\alpha\beta}s^{\alpha\beta}]\rangle$.

Using Eqs. (5) and (6), we find for the conductance

$$g\equiv\langle\mathrm{Tr}[s^{\dagger\alpha\beta}s^{\alpha\beta}]\rangle=\frac{1}{(4M)^2}\sum_{m,n}\frac{1}{k_m k_n}\int_{C_\alpha}dy_2dy_3\chi_n(y_2)\chi_n(y_3)\times\int_{C_\beta}dy_1dy_4\chi_m(y_1)\chi_m(y_4)[ik_m-\partial_{x_1}][-ik_n-\partial_{x_2}]\times[ik_n-\partial_{x_3}][-ik_m-\partial_{x_4}]\times\langle G^A(\boldsymbol{r}_1,\boldsymbol{r}_2)G^R(\boldsymbol{r}_3,\boldsymbol{r}_4)\rangle\big|^{x_1=x_4=L}_{x_2=x_3=0}, \quad (8)$$

where the Green's functions are taken at the Fermi energy. Since the averaged Green's functions decay on scales of the mean free path, the average product of two Green's functions, each of them taken in remote points, is due only to the diffusion (see, e.g., Ref. 31):

$$\langle G^A(\boldsymbol{r}_1,\boldsymbol{r}_2)G^R(\boldsymbol{r}_3,\boldsymbol{r}_4)\rangle=\int d\boldsymbol{r}_a d\boldsymbol{r}_b\langle G^A(\boldsymbol{r}_1,\boldsymbol{r}_a)\rangle\times\langle G^A(\boldsymbol{r}_b,\boldsymbol{r}_2)\rangle\langle G^R(\boldsymbol{r}_3,\boldsymbol{r}_b)\rangle\times\langle G^R(\boldsymbol{r}_a,\boldsymbol{r}_4)\rangle\times P(\boldsymbol{r}_a,\boldsymbol{r}_b). \quad (9)$$

The diffusion propagator $P(\boldsymbol{r},\boldsymbol{r}')$ is a solution of the equation

$$-D\nabla^2_{\boldsymbol{r}}P(\boldsymbol{r},\boldsymbol{r}')=(2\pi\nu\tau^2)^{-1}\delta(\boldsymbol{r}-\boldsymbol{r}') \quad (10)$$

with appropriate boundary conditions ($P=0$ at the contact to the ideal leads and $\boldsymbol{n}\nabla P=0$ at the walls). Here $\nu=M/2\pi$, $D=v_F l/2$, and τ are the density of states, the diffusion coefficient, and the elastic lifetime, respectively. Under the assumption $L\gg W$, the diffusion can be considered to be one dimensional and the diffusion propagator does not depend on y,

$$P(x,x')=(M\tau^2DWL)^{-1}\begin{cases}x(L-x'), & x<x'\\ x'(L-x), & x>x'.\end{cases} \quad (11)$$

Now we insert Eq. (9) into Eq. (8). The diagram for g is shown in Fig. 3. One can approximate the short-ranged Green's functions as

$$\langle G^R(\boldsymbol{r},\boldsymbol{r}')\rangle=-\frac{iM}{p_F}\exp\left[\left(ip_F-\frac{1}{2l}\right)|x-x'|\right]\delta(y-y'). \quad (12)$$

Then, integrating over transverse coordinates, we obtain

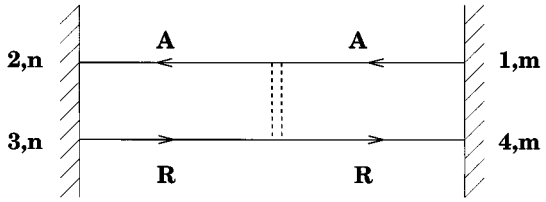

FIG. 3. Diagram for the conductance. The double dashed line represents the diffusion propagator. The position and the transverse channel number of the points on the surfaces C_α ($x=0$) and C_β ($x=L$) are shown. For example, the transverse wave function χ_m is taken at the point y_1.

$$g=\frac{M}{16D\tau^2LW}\left[\sum_m \frac{1}{k_m}\left(1+\frac{k_m}{p_F}\right)^2\right]^2\int_0^L dx_a dx_b \times\exp[-x_a/l]\exp[-(L-x_b)/l]x_a(L-x_b). \quad (13)$$

Taking into account that

$$\sum_m \frac{1}{k_m}\left(1+\frac{k_m}{p_F}\right)^2=2W,$$

we obtain

$$g=\frac{l}{2L}p_F W. \quad (14)$$

Multiplied by $e^2/2\pi$, Eq. (14) gives the Drude formula, as it should be.

B. Evaluation of $\langle \mathrm{Tr}[s^{\dagger\alpha\beta}s^{\alpha\beta}s^{\dagger\alpha\beta}s^{\alpha\beta}]\rangle$.

The trace of a product of four scattering matrices can be written as

$$\begin{aligned} t\equiv&\langle \mathrm{Tr}[s^{\dagger\alpha\beta}s^{\alpha\beta}s^{\dagger\alpha\beta}s^{\alpha\beta}]\rangle \\ =&\frac{1}{(4M)^4}\sum_{k,l,m,n}\frac{1}{k_k k_l k_m k_n}\int_{C_\alpha} dy_2 dy_3 dy_6 dy_7 \chi_l(y_2)\chi_l(y_3) \\ &\times\chi_n(y_6)\chi_n(y_7)\int_{C_\beta} dy_1 dy_4 dy_5 dy_8 \chi_k(y_1)\chi_m(y_4)\chi_m(y_5) \\ &\times\chi_k(y_8)[ik_k-\partial_{x_1}][-ik_l-\partial_{x_2}][ik_l-\partial_{x_3}][-ik_m-\partial_{x_4}] \\ &\times[ik_m-\partial_{x_5}][-ik_n-\partial_{x_6}][ik_n-\partial_{x_7}][-ik_k-\partial_{x_8}] \\ &\times\langle G^A(\boldsymbol{r}_1,\boldsymbol{r}_2)G^R(\boldsymbol{r}_3,\boldsymbol{r}_4)G^A(\boldsymbol{r}_5,\boldsymbol{r}_6) \\ &\times G^R(\boldsymbol{r}_7,\boldsymbol{r}_8)\rangle\big|_{x_2=x_3=x_6=x_7=0}^{x_1=x_4=x_5=x_8=L}. \end{aligned} \quad (15)$$

Employing Eq. (9) again, we find the diagrams shown in Fig. 4. We omitted all diagrams containing a single electron line connecting two different leads since these are exponentially small; the diagrams in Figs. 4(a) and 4(e) contain also counterparts, similar to Figs. 4(c) and 4(d).

The diagrams in Figs. 4(b)–4(d) turn out to give the leading contribution, whereas others carry small factors. Thus, for the diagram in Fig. 4(a) points y_1 and y_4 should lie not farther apart than a mean free path, which, due to the orthogonality of transverse wave functions, implies $k=m$. Therefore, the contribution of this diagram is suppressed by

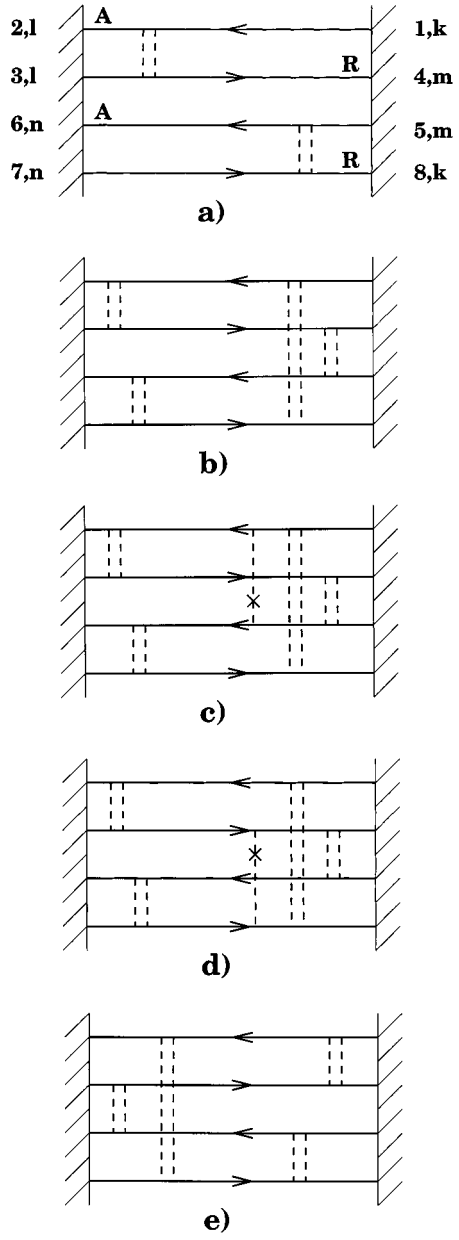

FIG. 4. Diagrams for the quantity t in the same notation as in Fig. 3. The single dashed line with a cross represents impurity scattering.

a factor $(p_F W)^{-1}\ll 1$. The diagram in Fig. 4(e), which is topologically equivalent to that in Fig. 4(b), is suppressed as $(p_F W)^{-3}$. Taking into account the explicit form (11) for the diffusion propagator and integrating over coordinates y_i and over one of two pair of coordinates in the diffusion propagators (those lying close to one of the ends of the wire), we arrive at the expression

$$t=\frac{l^8}{2(4D\tau^2WL)^4}\left[\sum_m \frac{1}{k_m}\left(1+\frac{k_m}{p_F}\right)^2\right]^4\int d\boldsymbol{r}_a d\boldsymbol{r}_b d\boldsymbol{r}_c d\boldsymbol{r}_d \times(L-x_a)(L-x_c)x_b x_d F(\boldsymbol{r}_a,\boldsymbol{r}_b,\boldsymbol{r}_c,\boldsymbol{r}_d). \quad (16)$$

Here F is the Hikami box.[32] It is short ranged (all points $\boldsymbol{r}_a$, $\boldsymbol{r}_b$, $\boldsymbol{r}_c$, and $\boldsymbol{r}_d$ should be close to each other) and in the Fourier space has the form

$$F(\boldsymbol{q}_a,\boldsymbol{q}_b,\boldsymbol{q}_c,\boldsymbol{q}_d)=-M\tau^5 v_F^2(2\pi)^2\delta(\boldsymbol{q}_a+\boldsymbol{q}_b+\boldsymbol{q}_c+\boldsymbol{q}_d)\times[2(\boldsymbol{q}_a\boldsymbol{q}_c+\boldsymbol{q}_b\boldsymbol{q}_d)+(\boldsymbol{q}_a+\boldsymbol{q}_c)(\boldsymbol{q}_b+\boldsymbol{q}_d)]. \tag{17}$$

Integration of the Hikami box over the cross section of the wire yields

$$\int F(\boldsymbol{r}_a,\boldsymbol{r}_b,\boldsymbol{r}_c,\boldsymbol{r}_d)dy_a dy_b dy_c dy_d = M\tau^5 v_F^2 W[2\partial_{x_a}\partial_{x_c}+2\partial_{x_b}\partial_{x_d}+\partial_{x_a}\partial_{x_b}+\partial_{x_a}\partial_{x_d}+\partial_{x_b}\partial_{x_c}+\partial_{x_c}\partial_{x_d}]\times\delta(x_a-x_b)\,\delta(x_a-x_c)\,\delta(x_a-x_d). \tag{18}$$

Inserting Eq. (18) into Eq. (16) and performing the remaining integrations, we obtain

$$t=\frac{l}{3L}p_F W=2g/3, \tag{19}$$

which immediately gives the 1/3 shot-noise suppression.

C. Universality

Now we lift the requirement $L\gg W$, but still consider a diffusive system $W,L\gg l$. The result (14) for $g=\langle \mathrm{Tr}[s^{\dagger\alpha\beta}s^{\alpha\beta}]\rangle$ is equivalent, in fact, to the Drude formula and is therefore valid for an arbitrary relation between W and L. In the derivation of $t=\langle \mathrm{Tr}[s^{\dagger\alpha\beta}s^{\alpha\beta}s^{\dagger\alpha\beta}s^{\alpha\beta}]\rangle$ we should now take into account that the diffusion is not one-dimensional anymore and write the diffusion propagator in the form

$$P(\boldsymbol{r},\boldsymbol{r}')=\frac{1}{M\tau^2 D}\sum_{\boldsymbol{q}}\frac{1}{q^2}\phi_{\boldsymbol{q}}(\boldsymbol{r})\phi_{\boldsymbol{q}}(\boldsymbol{r}') \tag{20}$$

instead of Eq. (11). Here $\phi_{\boldsymbol{q}}(\boldsymbol{r})$ and $-q^2$ are eigenfunctions and eigenvalues of the Laplace operator with appropriate boundary conditions. In our particular geometry one obtains

$$\boldsymbol{q}=\left(\frac{\pi}{L}n_x,\frac{\pi}{W}n_y\right),$$

with integers $n_x>0$ and $n_y\geq 0$. It is easy to see that the integration over y_1 and y_8 in the diagrams of Figs. 4(b)–4(d) places a constraint on the wave vector n_{1y} of the diffusion propagator connecting these two points $n_{1y}=2k$ (unless $n_{1y}=0$). In the same way, the other integrations over y_i imply other constraints, which, due to the δ function in the expression for the Hikami box (17), yield a constraint on the channel indices k,l,m,n. Therefore, all terms with nonzero transverse harmonics are as small as $(p_F W)^{-1}$. Up to terms proportional to this small parameter the result (19) is exact. Thus the 1/3 shot-noise suppression is indeed universal and does not depend on the ratio W/L, provided the system is diffusive, in accordance with the conclusion of Ref. 5.

To conclude this section, we compare the method used above with other derivations of the 1/3 shot-noise suppression.[2–4] As is well known, there exist two principally different methods of calculating conductance. One can first evaluate conductivity (which is a local quantity), starting from the Kubo formula, and then, after integration over a cross section, one obtains the conductance. Alternatively, one can calculate conductance directly, starting from the Landauer formula. (In fact, our derivation of the quantity g given above is of this kind.) Both derivations are equivalent, although at intermediate stages they do not have much in common.

A similar situation happens in the calculation of shot noise. On the one hand, one can calculate the microscopic correlator of currents and upon integration over a cross section obtain the shot noise power. The derivation of Altshuler, Levitov, and Yakovets[4] is exactly of this type.[33] It can be generalized to an arbitrary geometry and, in principle, can be used for a broad class of problems. The local current correlator contains more information than is necessary for the calculation of the shot-noise power. The method of Nagaev[3] and de Jong and Beenakker,[7] who employ the Langevin equation, is somewhat similar, although the equivalence between these two approaches (Ref. 4 and Refs. 3 and 7) is not evident. The generalization of the latter approach for a multiterminal geometry does not seem to be quite obvious.

The derivation of Beenakker and one of the authors (M.B.),[2] as well as the present method, belong to another, scattering (or Landauer) type of approach. Reference 2 derives the shot-noise power with the use of the distribution of transmission eigenvalues of the diffusive wire. This proof seems to be the most elegant. However, one should not forget that the distribution of transmission eigenvalues itself is derived by sophisticated methods such as the Dorokhov-Mello-Pereyra-Kumar equation.[34] Although Nazarov[5] succeeded in extending this derivation to the case of an arbitrary two-terminal geometry, most probably it cannot be generalized to the multiterminal case: For conductors with four (or more) probes the shot noise is not expressed through eigenvalues of the scattering matrix $s^\dagger s$. The derivation given in this paper is more general and self-contained; it does not require the distribution of transmission eigenvalues and hence allows a generalization to an arbitrary scattering geometry.

Our derivation resembles in some respects those of Refs. 4 and 7. In particular, de Jong and Beenakker[7] at some stage express the scattering matrix $s^{\dagger\alpha\beta}s^{\alpha\beta}$ through the Green's function and proceed with impurity averaging. We should stress, however, that their semiclassical approach does not take into account phase-sensitive effects (exchange terms), in contrast to the approach presented here. In addition, even at the semiclassical level the equivalence between these two discussions is not evident.

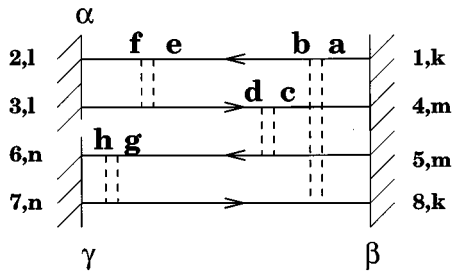

FIG. 5. Typical diagram for the quantity Ξ_1.

III. MULTITERMINAL SHOT NOISE

Now we turn to the exchange-interference experiment described in the Introduction. We consider a four-terminal geometry (examples are shown in Fig. 1; for convenience, we still use the coordinates of Fig. 2) and calculate the current correlation for experiments A–C.

The quantity $\Xi_1=\mathrm{Tr}(s^{\dagger\alpha\beta}s^{\alpha\beta}s^{\dagger\gamma\beta}s^{\gamma\beta})$ is determined by the diagrams of Fig. 4, where now points y_1,y_4,y_5,y_8 belong to the contact with lead β; points y_2,y_3 and y_6,y_7 belong to the contacts with leads α and γ, respectively. Therefore, the diagram in Fig. 4(e) is exponentially small, while the diagram in Fig. 4(a) is suppressed in the parameter $(p_F W_\beta)^{-1}$. Hence the quantity Ξ_1 is given by the same diagrams [Figs. 4(b)–4(d)], as the quantity t. Using Eq. (12) and integrating over the cross section of the leads, we obtain (Fig. 5)

$$\Xi_1=\frac{1}{2}\left(\frac{M}{4}\right)^4\sum_{k,l,m,n}\frac{1}{k_k k_l k_m k_n}\left(1+\frac{k_k}{p_F}\right)^2\left(1+\frac{k_l}{p_F}\right)^2\left(1+\frac{k_m}{p_F}\right)^2\left(1+\frac{k_n}{p_F}\right)^2\int_{C_\alpha}dy_f\chi_l^2(y_f)\int_{C_\beta}dy_a dy_c\chi_k^2(y_a)\chi_m^2(y_c)$$
$$\times\int_{C_\gamma}dy_h\chi_n^2(y_h)\int_{-\infty}^{0}dx_a dx_c dx_f dx_h\exp[(x_a+x_c+x_f+x_h)/l]\int d\boldsymbol{r}_a\cdots d\boldsymbol{r}_h P(\boldsymbol{r}_a,\boldsymbol{r}_b)P(\boldsymbol{r}_c,\boldsymbol{r}_d)$$
$$\times P(\boldsymbol{r}_e,\boldsymbol{r}_f)P(\boldsymbol{r}_g,\boldsymbol{r}_h)F(\boldsymbol{r}_b,\boldsymbol{r}_e,\boldsymbol{r}_d,\boldsymbol{r}_g). \tag{21}$$

Here the points $\boldsymbol{r}_a,\boldsymbol{r}_c,\boldsymbol{r}_f,\boldsymbol{r}_h$ are given in the coordinates of the contacts $\beta,\beta,\alpha,\gamma$, respectively.

In the same way, for the quantity Ξ_3 one obtains

$$\Xi_3=\frac{1}{2}\left(\frac{M}{4}\right)^4\sum_{k,l,m,n}\frac{1}{k_k k_l k_m k_n}\left(1+\frac{k_k}{p_F}\right)^2\left(1+\frac{k_l}{p_F}\right)^2\left(1+\frac{k_m}{p_F}\right)^2\left(1+\frac{k_n}{p_F}\right)^2\int_{C_\alpha}dy_f\chi_l^2(y_f)\int_{C_\beta}dy_a\chi_k^2(y_a)\int_{C_\gamma}dy_h\chi_n^2(y_h)$$
$$\times\int_{C_\delta}dy_c\chi_m^2(y_c)\int_{-\infty}^{0}dx_a dx_c dx_f dx_h\exp[(x_a+x_c+x_f+x_h)/l]$$
$$\times\int d\boldsymbol{r}_a\cdots d\boldsymbol{r}_h P(\boldsymbol{r}_a,\boldsymbol{r}_b)P(\boldsymbol{r}_c,\boldsymbol{r}_d)P(\boldsymbol{r}_e,\boldsymbol{r}_f)P(\boldsymbol{r}_g,\boldsymbol{r}_h)F(\boldsymbol{r}_b,\boldsymbol{r}_e,\boldsymbol{r}_d,\boldsymbol{r}_g) \tag{22}$$

and the points $\boldsymbol{r}_a,\boldsymbol{r}_c,\boldsymbol{r}_f,\boldsymbol{r}_h$ are given in the coordinates of the contacts $\beta,\delta,\alpha,\gamma$, respectively. Expressions for the quantities Ξ_2 and Ξ_4 can be obtained from Eqs. (21) and (22), respectively, by interchanging $\beta\leftrightarrow\delta$.

Expressions (21) and (22) are valid for an arbitrary four-terminal geometry and can be used for numerical calculations. It is important that not only traces Ξ_1 and Ξ_2, as one could expect, but also quantities Ξ_3 and Ξ_4 are phase insensitive. Indeed, the electron motion that Eqs. (21) and (22) imply is just the diffusion between different leads. No closed paths are formed, except for ballistic motion due to the scattering described by the Hikami box somewhere in the middle of the sample. Since the size of this loop is very small, of the order of the mean free path, dephasing is not expected to have an effect on the exchange noise. Certainly, some effects similar to weak localization exist, however, as for conductance,[31] they are relatively weak [as $(p_F l)^{-1}$] in comparison to the main effect. We do not discuss these effects here and only mention that universal fluctuations of the shot noise were studied in Ref. 35.

To make further progress we have to solve the diffusion equation in a given geometry with appropriate boundary conditions. We turn now to the two different geometries, shown in Fig. 1.

A. Box geometry

First, we consider the geometry of Fig. 1(a). We assume all leads to be wide $W_\lambda\gg l$. Then points $\boldsymbol{r}_a$, $\boldsymbol{r}_c$, $\boldsymbol{r}_f$, and $\boldsymbol{r}_h$ are typically far from the lead's boundaries. This means, for example, that in the integral over y_f one can replace the diffusion propagator $P(\boldsymbol{r}_e,\boldsymbol{r}_f)$ by another function $\tilde{P}(\boldsymbol{r}_e,\boldsymbol{r}_f)$, which is also a solution to the diffusion equation, but with another boundary condition, appropriate for an open surface,

$$\tilde{P}(\boldsymbol{r},\boldsymbol{r}')|_{x=0}=0.$$

We do not need to specify boundary conditions for $\tilde{P}(\boldsymbol{r}_e,\boldsymbol{r}_f)$ on the other boundaries since the point $\boldsymbol{r}_e$ is typically in the middle of the sample. Consequently, we may substitute for all ''true'' diffusion propagators P the functions $\tilde{P}$, the solution with $\tilde{P}=0$ everywhere on the boundary, as is appropriate for an open system. The solution $\tilde{P}$ is

$$\tilde{P}(\boldsymbol{r},\boldsymbol{r}')=\frac{4}{M\tau^2 D L_x L_y}\sum_{n_x,n_y=1}^{\infty}\frac{1}{\pi^2 n_x^2/L_x^2+\pi^2 n_y^2/L_y^2}\sin\frac{\pi n_x x}{L_x}$$
$$\times\sin\frac{\pi n_x x'}{L_x}\sin\frac{\pi n_y y}{L_y}\sin\frac{\pi n_y y'}{L_y}. \tag{23}$$

Furthermore, the functions $\tilde{P}$ vary considerably on the scale of the size of a sample L_x and L_y. If we assume $W_\lambda\ll L_x,L_y$, the function $\tilde{P}(\boldsymbol{r}_e,\boldsymbol{r}_f)$ in the integral over y_f may be taken to be independent of y_f. Thus we obtain

$$\Xi_1=\frac{1}{2}\left(\frac{M}{2}\right)^4 W_\alpha W_\beta^2 W_\gamma \int dy_a dy_c dx_f dx_h \exp\left(-\frac{L_y-y_a}{l}-\frac{L_y-y_c}{l}-\frac{x_f}{l}-\frac{L_x-x_h}{l}\right)\int d\boldsymbol{r}_b d\boldsymbol{r}_d d\boldsymbol{r}_e d\boldsymbol{r}_g \times\widetilde{P}[X_\beta,y_a;\boldsymbol{r}_b]\widetilde{P}[X_\beta,y_c;\boldsymbol{r}_d]\widetilde{P}[\boldsymbol{r}_e;x_f,Y_\alpha] \times\widetilde{P}[\boldsymbol{r}_g;x_h,Y_\gamma]F(\boldsymbol{r}_b,\boldsymbol{r}_e,\boldsymbol{r}_d,\boldsymbol{r}_g) \tag{24}$$

and

$$\Xi_3=\frac{1}{2}\left(\frac{M}{2}\right)^4 W_\alpha W_\beta W_\gamma W_\delta \int dy_a dy_c dx_f dx_h \exp\left(-\frac{L_y-y_a}{l}-\frac{y_c}{l}-\frac{x_f}{l}-\frac{L_x-x_h}{l}\right)\int d\boldsymbol{r}_b d\boldsymbol{r}_d d\boldsymbol{r}_e d\boldsymbol{r}_g \widetilde{P}[X_\beta,y_a;\boldsymbol{r}_b] \times\widetilde{P}[X_\delta,y_c;\boldsymbol{r}_d]\widetilde{P}[\boldsymbol{r}_e;x_f,Y_\alpha]\widetilde{P}[\boldsymbol{r}_g;x_h,Y_\gamma] \times F(\boldsymbol{r}_b,\boldsymbol{r}_e,\boldsymbol{r}_d,\boldsymbol{r}_g). \tag{25}$$

Here Y_α, X_β, Y_γ, and X_δ denote the positions of the corresponding leads.

We see already from Eqs. (24) and (25) that the results are not universal in the sense that they depend on the geometry of the sample. Indeed, within the approximation in which we replace P by $\widetilde{P}$, the quantity Ξ_1 does not contain any information on the location and width of lead δ; at the same time, it depends essentially on the location and width of other leads. The quantity Ξ_2 contains information of all leads except β, whereas both Ξ_3 and Ξ_4 are governed by the geometry of all leads. Therefore, all ratios Ξ_i/Ξ_j depend essentially on the geometry of the sample. This is in contrast with the case of a chaotic cavity,[18] where one obtains $\Xi_1=\Xi_2=-3\Xi_3=-3\Xi_4$ irrespective of geometry, provided the leads are wide enough.

Performing the integration and taking into account that the remaining sums are converging rapidly for $L_x\sim L_y$ (the case we assume from now on), one obtains cumbersome expressions for the quantities Ξ_i. In the symmetric case $L_x=L_y=L$, $W_\lambda=W$, and $Y_\alpha=Y_\gamma=X_\beta=X_\delta=L/2$ they simplify. We obtain

$$\begin{Bmatrix}\Xi_1=\Xi_2\\ \Xi_3=\Xi_4\end{Bmatrix}=\begin{Bmatrix}\eta_1\\ -\eta_3\end{Bmatrix}p_F l\left(\frac{W}{L}\right)^4, \tag{26}$$

with positive constants

$$\eta_1=\frac{1}{2\sinh^3\pi}(\cosh\pi-1)(2\pi\cosh\pi-\sinh\pi)\approx 0.21$$

and

$$\eta_3=\frac{1}{\sinh^3\pi}(2\pi\cosh\pi-\sinh\pi)\approx 0.03.$$

It is seen that the exchange effect exists and has a *negative* sign (i.e., exchange suppresses the result of experiment C in comparison to the sum of the results of experiments A and B). Although the relative value of the effect is $\Xi_3/\Xi_1\sim 0.1$, the effect should be clearly observable.

B. Cross geometry

We consider now the cross geometry of Fig. 1(b). We assume that all arms of the cross have equal[36] lengths L and widths W. For $L\gg W$ we can consider diffusion as one dimensional. We also assume that the center of the cross is described by a reflection coefficient R and a transmission coefficient $T=(1-R)/3$ between any two different arms.

The diffusion propagator is a solution of Eq. (10). We move to the coordinate system of Fig. 1(b) and fix the point $\boldsymbol{r}$ near the origin of the lead α, $x\simeq L$. We introduce

$$P_{\alpha\lambda}(x,x')=P(x,x') \quad \text{if } x' \text{ lies in the arm } \lambda,$$

which is proportional to the time-integrated probability of diffusion from point x in the arm α to point x' in the arm λ. The solution satisfying the boundary conditions and the condition of current conservation in the cross,

$$\sum_\lambda \partial_{x'}P_{\alpha\lambda}(x,x')|_{x'=0}=0,$$

is

$$P_{\alpha\alpha}(x,x_\alpha)=\frac{1}{MD\tau^2 W}\frac{(L-x)(L\epsilon+3x_\alpha)}{3+\epsilon}, \quad x>x_\alpha$$

$$P_{\alpha\lambda}(x,x_\lambda)=\frac{1}{MD\tau^2 W}\frac{(L-x)(L-x_\lambda)}{3+\epsilon}, \quad \lambda\neq\alpha. \tag{27}$$

The constant ϵ, defined as the ratio of diffusion probabilities

$$\epsilon=\frac{P_{\alpha\alpha}(x,0)}{P_{\alpha\beta}(x,0)}, \tag{28}$$

is calculated in the Appendix. The result is

$$\epsilon=\begin{cases}1+l(LT)^{-1}(1-2T), & T\gg l/L\\ l(LT)^{-1}, & T\ll l/L.\end{cases} \tag{29}$$

Now we substitute Eq. (27) into the general expressions (21) and (22). Since the area of the cross is negligible in comparison to the areas of the arms, we can neglect the possibility of finding the Hikami box inside the cross and allow it to be situated only in one of the arms. Upon integration we obtain

$$\Xi_1=\Xi_2=\frac{l}{3L}Wp_F\frac{3(1+\epsilon^2)+4}{(3+\epsilon)^4},$$

$$\Xi_3=\Xi_4=\frac{4l}{L}Wp_F\frac{\epsilon-1}{(3+\epsilon)^4}. \tag{30}$$

Thus, in the case $T\gg l/L$, when the overall transmission through the sample is governed by the diffusive arms rather than by the center of the cross, one has $\epsilon\sim 1$. The quantities Ξ_1 and Ξ_2 are regular for $\epsilon=1$ and therefore assume the finite value $\Xi_1=\Xi_2=(5/192)(p_F Wl/L)$. At the same time, the exchange terms Ξ_3 and Ξ_4 are strongly suppressed in the parameter l/L, $\Xi_3=\Xi_4=(1/64)(p_F Wl^2/L^2T)(1-2T)$. In the less realistic case $T\ll l/L$ (the transmission is determined by the center of the cross) one obtains $\epsilon\gg 1$. All quantities Ξ_1 are small since now all channels are nearly closed (cf. the

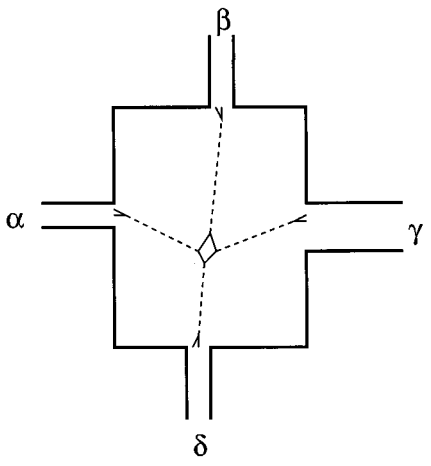

FIG. 6. Typical electron trajectories, contributing to the quantity Ξ_3. Solid lines denote ballistic propagation (described by averaged single-particle Green's function) and dashed lines denote diffusive propagation (described by the diffusion P).

situation for two-terminal shot noise[29,30]); however exchange terms are additionally suppressed in the parameter ϵ^{-1}.

Thus, in the cross geometry of Fig. 1(b) the exchange noise $\langle \Delta S \rangle$ is suppressed in comparison to the regular terms $\langle S_A + S_B \rangle$ irrespective of the transmission properties of the center of the cross. It is also quite remarkable that for the cross geometry the exchange contribution is *positive*, although small: The total effect is enhanced by the exchange.

IV. CONCLUSION

We have investigated shot noise in diffusive conductors on the basis of Eq. (2) and the Fisher-Lee relation, which expresses scattering matrices through advanced and retarded Green's functions. In this way, one can reduce disorder averages of various combinations of scattering matrices to standard diagram technique for Green's functions.[31] Although this approach resembles previously published calculations of conductance and conductance fluctuations,[24–28] we believe it to be more transparent. We are not aware of any applications of this approach to noise problems.

As a check of the method, we first reproduced the 1/3 shot-noise suppression in the two-terminal geometry and confirmed the statement of Ref. 5 that it is in fact superuniversal and holds for an arbitrary relation between the length and width of a wire, provided the system is diffusive. Our proof bears some similarity to other ones existing in the literature;[2–4] however, it is different, and a direct equivalence to any of the existing proofs is not evident (see the discussion at the end of Sec. II).

Then we turned to the multiterminal geometry and investigated the interference experiment, similar to the Hanbury Brown–Twiss experiment known in optics.[15] We obtained general expressions for scattering matrix combinations (21) and (22), determining noise intensities (1); then we investigated them for the two different geometries of Fig. 1.

The important point we make is that the exchange effect, even when averaged over disorder, does not vanish. The reason is that typical electron trajectories, contributing to *all*

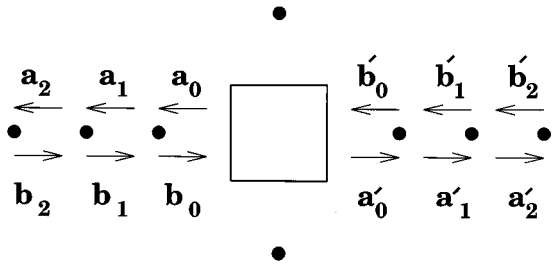

FIG. 7. Discrete diffusion model.

averaged traces of scattering matrices, considered above (i.e., quantities g and t for the two-terminal geometry and Ξ_i in the four-terminal case) do not contain large closed loops. In particular, it is valid for the ''exchange'' traces Ξ_3 and Ξ_4. A typical trajectory for the quantity Ξ_3 is shown in Fig. 6. It is a direct translation of diagrams contributing to this quantity. The electron motion is essentially diffusion between different leads with ballistic propagation (described by disorder-averaged single-particle Green's function) close to the leads and somewhere in the middle of the sample [the later motion described by the Hikami box in Eq. (22)]. Thus closed loops are related to ballistic motion over distances of an elastic scattering length only and therefore neither the shot noise in two-terminal conductors nor the shot noise in multiterminal structures should be sensitive to dephasing.

Another observation is that exchange corrections are not universal, in contrast to what is found in the chaotic case:[18] The ratio $\langle \Delta S \rangle / \langle S_A + S_B \rangle$ depends on the geometry of a sample in an essential way. Even the sign of the effect may change: For the box geometry of Fig. 1(a) it is negative, i.e., interference suppresses the total effect, while for the cross geometry [Fig. 1(b)] interference enhances the effect (although weakly).

The results obtained for the cross geometry allow us to make predictions for experiments in real systems. Indeed, we found that the exchange contribution is suppressed strongly with respect to the average noise intensities $\langle S_A \rangle$ and $\langle S_B \rangle$. This result was obtained by assuming that the intermediate scattering, described by the Hikami box, does not happen in the center of the cross, i.e., strictly speaking, for ballistic propagation through the center. In more complicated situations the entire exchange effect will be determined by properties of the center of the cross. If the motion within the center is diffusive, one can apply the results obtained above for the box geometry. The total exchange effect is expected to be negative. However, since the arms of the cross (which correspond to disordered leads in the real experiments) contribute to the intensities $\langle S_A \rangle$ and $\langle S_B \rangle$, but not to the exchange contribution, the latter will still be suppressed if disorder extends far into leads. Finally, if the center of the cross is a chaotic cavity, one may use the results of Ref. 18. The exchange contribution in the chaotic cavity separated from ideal leads by high barriers (disordered arms play the role of these barriers) is positive: The interference enhances the effect.

ACKNOWLEDGMENTS

We thank S. van Langen, who calculated the exchange-interference correlator for chaotic cavities, for useful discus-

sions. The work was supported by the Swiss National Science Foundation.

APPENDIX

To find the coefficient ϵ defined by Eq. (28) it is instructive to consider a discrete model of diffusion.[37] Each arm is modeled by a one-dimensional array of scatterers, placed at a distance l from each other; the total number of scatterers in each arm is $N=L/l$. Each scatterer is described by transmission $t=1/2$ and reflection $r=1/2$ probabilities. We denote the carrier flux densities in the arm α between sites n and $n+1$ away from the center of the cross by a_n and the flux towards the center of the cross by b_n. Corresponding amplitudes in other arms are denoted by a'_n and b'_n (Fig. 7). The total flux at each site is given by $\rho_n=a_n+b_n$ and $\rho'_n=a'_n+b'_n$. The coefficient ϵ can be expressed as $\epsilon=\rho_0/\rho'_0$.

The diffusion equation implies that all densities should be linear functions of n; furthermore, matching conditions at each scatterer require $b_{n-1}=a_n$ and $b'_{n-1}=a'_n$. Thus we write

$$a_n=A+B(n-1), \quad a'_n=A'+B'(n-1), \tag{A1}$$

$$b_n=A+Bn, \quad b'_n=A'+B'n. \tag{A2}$$

The four constants A,B,A',B' obey four equations: (i) the boundary condition for the arm β, $b'_N=0$; (ii) and (iii) the matching conditions at the center of the cross,

$$a'_0=Tb_0+2Tb'_0+Rb_0 \tag{A3}$$

and

$$a_0=3Tb'_0+Rb_0; \tag{A4}$$

and (iv) Eq. (10), which, however, it is not required for the calculation of the constant ϵ. We obtain

$$\epsilon=\frac{2(N+T^{-1})-3}{2N+1} \tag{A5}$$

and the limiting cases given by Eq. (29) follow immediately.

[1] For a review of shot noise in electron systems, see M. J. M. de Jong and C. W. J. Beenakker, in *Mesoscopic Electron Transport, NATO Advanced Study Institute, Series E: Applied Science*, edited by L. P. Kouwenhoven, G. Schön, and L. L. Sohn (Kluwer, Dordrecht, in press).

[2] C. W. J. Beenakker and M. Büttiker, Phys. Rev. B **46**, 1889 (1992).

[3] K. E. Nagaev, Phys. Lett. A **169**, 103 (1992).

[4] B. L. Altshuler, L. S. Levitov, and A. Yu. Yakovets, Pis'ma Zh. Eksp. Teor. Fiz. **59**, 821 (1994) [JETP Lett. **59**, 857 (1994)].

[5] Yu. V. Nazarov, Phys. Rev. Lett. **73**, 134 (1994).

[6] F. Liefrink, J. I. Dijkhuis, M. J. M. de Jong, L. W. Molenkamp, and H. van Houten, Phys. Rev. B **49**, 14 066 (1994). The suppression observed in this experiment varies between 0.2 and 0.4 and is voltage dependent. As suggested in Refs. 10 and 8, the observed effect can be due to the noise caused by electron heating.

[7] M. J. M. de Jong and C. W. J. Beenakker, Phys. Rev. B **51**, 16 867 (1995); Physica A **230**, 219 (1996).

[8] A. H. Steinbach, J. M. Martinis, and M. H. Devoret, Phys. Rev. Lett. **76**, 3806 (1996).

[9] K. E. Nagaev, Phys. Rev. B **52**, 4740 (1995).

[10] V. I. Kozub and A. M. Rudin, Phys. Rev. B **52**, 7853 (1995).

[11] A. Shimizu and M. Ueda, Phys. Rev. Lett. **69**, 1403 (1992).

[12] R. Landauer, Ann. (N.Y.) Acad. Sci. **755**, 417 (1995); Physica B **227**, 156 (1996).

[13] R. C. Liu and Y. Yamamoto, Phys. Rev. B **60**, 17 411 (1994); **53**, 7555(E) (1994).

[14] M. Büttiker, Phys. Rev. B **46**, 12 485 (1992).

[15] R. Hanbury Brown and R. Q. Twiss, Nature (London) **177**, 27 (1956); M. L. Goldberger, H. W. Lewis, and K. M. Watson, Phys. Rev. **132**, 2764 (1963); R. Loudon, in *Disorder in Condensed Matter Physics*, edited by J. A. Blackman and J. Taguena (Clarendon, Oxford, 1991), p. 441.

[16] We set $\omega=T=0$ and discuss only the regime linear in voltage V throughout the paper. We also set $\hbar=1$.

[17] Current correlations in normal conductors are quite generally negative (see Ref. 14). Thus S_j, as defined here, are positive quantities in normal conductors. In contrast, in hybrid normal and superconducting structures the current-current correlations can change sign. See M. P. Anantram and S. Datta, Phys. Rev. B **53**, 16 390 (1996); T. Martin, Phys. Lett. A **220**, 137 (1996).

[18] S. van Langen and M. Büttiker, cond-mat/9702067 (unpublished).

[19] F. von Oppen and A. Stern, LANL Report No. 079, cond-mat/9611079 (unpublished).

[20] D. S. Fisher and P. A. Lee, Phys. Rev. B **23**, 6851 (1981).

[21] A. D. Stone and A. Szafer, IBM J. Res. Dev. **32**, 384 (1988).

[22] H. U. Baranger and A. D. Stone, Phys. Rev. B **40**, 8169 (1989).

[23] A. A. Abrikosov, L. P. Gor'kov, and I. E. Dzyaloshinski, *Methods of Quantum Field Theory in Statistical Physics* (Prentice-Hall, Englewood Cliffs, New Jersey 1963).

[24] S. Iida, H. A. Weidenmüller, and J. A. Zuk, Ann. Phys. (N.Y.) **200**, 219 (1990).

[25] A. Altland, Z. Phys. B **82**, 105 (1991).

[26] S. Iida and A. Müller-Groeling, Phys. Rev. B **44**, 8097 (1991).

[27] A. Müller-Groeling, Phys. Rev. B **47**, 6480 (1993).

[28] A. D. Mirlin, A. Müller-Groeling, and M. R. Zirnbauer, Ann. Phys. (N.Y.) **236**, 325 (1994).

[29] M. Büttiker, Phys. Rev. Lett. **65**, 2901 (1990).

[30] V. A. Khlus, Zh. Eksp. Teor. Fiz. **93**, 2179 (1987) [Sov. Phys. JETP **66**, 1243 (1987)]; G. B. Lesovik, Pis'ma Zh. Eksp. Teor. Fiz. **49**, 513 (1989) [JETP Lett. **49**, 592 (1989)].

[31] B. L. Altshuler and A. G. Aronov, in *Electron-Electron Interactions in Disordered Systems*, edited by A. L. Efros and M. Pollak (North-Holland, Amsterdam, 1985), p. 1.

[32] S. Hikami, Phys. Rev. B **24**, 2671 (1981).

[33] This derivation is close to the calculation of fluctuations of current-voltage characteristics in mesoscopic conductors, A. I. Larkin and D. E. Khmel'nitskii, Zh. Eksp. Teor. Fiz. **91**, 1815 (1986) [Sov. Phys. JETP **64**, 1075 (1986)].

[34] O. N. Dorokhov, Pis'ma Zh. Eksp. Teor. Fiz. **36**, 259 (1982) [JETP Lett. **36**, 318 (1982)]; P. A. Mello, P. Pereyra, and N. Kumar, Ann. Phys. (N.Y.) **181**, 290 (1988).

[35] M. J. M. de Jong and C. W. J. Beenakker, Phys. Rev. B **46**, 13 400 (1992).

[36] Generalization to arbitrary geometry is trivial provided $L \gg W$ and does not lead to any qualitatively new results.

[37] A similar approach was used to investigate the time of diffusion by R. Landauer, M. Büttiker, Phys. Rev. B **36**, 6255 (1987), and for the description of the dephasing electrode by M. Büttiker, *ibid.* **35**, 4123 (1987).